

Interesting Images

Photoacoustic Tomography Appearance of Fat Necrosis: A First-in-Human Demonstration of Biochemical Signatures along with Histological Correlation

Yonggeng Goh ^{1,†}, Ghayathri Balasundaram ^{2,†}, Hui Min Tan ³ , Thomas Choudary Putti ³, Celene Wei Qi Ng ⁴, Eric Fang ¹, Renzhe Bi ² , Siau Wei Tang ⁴, Shaik Ahmad Buhari ⁴, Mikael Hartman ⁴, Ching Wan Chan ⁴, Yi Ting Lim ¹, Malini Olivo ^{2,*} and Swee Tian Quek ^{1,*}

¹ Department of Diagnostic Imaging, National University Hospital, 5 Lower Kent Ridge Road, Singapore 119074, Singapore

² Translational Biophotonics Laboratory, Institute of Bioengineering & Bioimaging, Agency for Science, Technology & Research, 11 Biopolis Way, #02-02 Helios, Singapore 138667, Singapore

³ Department of Pathology, National University Hospital, 5 Lower Kent Ridge Road, Singapore 119074, Singapore

⁴ Department of Breast Surgery, National University Hospital, 5 Lower Kent Ridge Road, Singapore 119074, Singapore

* Correspondence: malini_olivo@ibb.a-star.edu.sg (M.O.); swee_tian_quek@nuhs.edu.sg (S.T.Q.); Tel.: +65-6478 7018 (M.O.)

† These authors contributed equally to this work.



Citation: Goh, Y.; Balasundaram, G.; Tan, H.M.; Putti, T.C.; Ng, C.W.Q.; Fang, E.; Bi, R.; Tang, S.W.; Buhari, S.A.; Hartman, M.; et al. Photoacoustic Tomography Appearance of Fat Necrosis: A First-in-Human Demonstration of Biochemical Signatures along with Histological Correlation. *Diagnostics* **2022**, *12*, 2456. <https://doi.org/10.3390/diagnostics12102456>

Academic Editor: Viktor Dremin

Received: 20 September 2022

Accepted: 10 October 2022

Published: 11 October 2022

Publisher's Note: MDPI stays neutral with regard to jurisdictional claims in published maps and institutional affiliations.



Copyright: © 2022 by the authors. Licensee MDPI, Basel, Switzerland. This article is an open access article distributed under the terms and conditions of the Creative Commons Attribution (CC BY) license (<https://creativecommons.org/licenses/by/4.0/>).

Abstract: A 50-year-old woman with no past medical history presented with a left anterior chest wall mass that was clinically soft, mobile, and non-tender. A targeted ultrasound (US) showed findings suggestive of a lipoma. However, focal “mass-like” nodules seen within the inferior portion suggested malignant transformation of a lipomatous lesion called for cross sectional imaging, such as MRI or invasive biopsy or excision for histological confirmation. A T1-weighted image demonstrated a large lipoma that has a central fat-containing region surrounded by an irregular hypointense rim in the inferior portion, confirming the benignity of the lipoma. An ultrasound-guided photoacoustic imaging (PA) of the excised specimen to derive the biochemical distribution demonstrated the “mass-like” hypoechoic regions on US as fat-containing, suggestive of benignity of lesion, rather than fat-replacing suggestive of malignancy. The case showed the potential of PA as an adjunct to US in improving the diagnostic confidence in lesion characterization.

Keywords: photoacoustic; lipoma; ultrasound; MRI

Fat necrosis, or cell death of adipose tissue, is a common benign condition that occurs from the lack of oxygen supply to adipose tissue [1]. As common causes include trauma or post-surgical changes [2], fat necrosis often presents as a palpable soft tissue mass at superficial regions [3].

Ultrasound (US) is the first-line imaging tool for these superficial lesions, but imaging appearances are extremely varied [4] due to the age of the lesion, which manifests as varying degrees of hardening, fibrosis, and degeneration. This often results in a diagnostic dilemma, which necessitates further cross-sectional imaging or invasive procedures, such as biopsy or excision for histological confirmation (Figures 1 and 2). There is, hence, an unmet clinical need for an adjunct imaging modality to US to improve diagnostic capability.

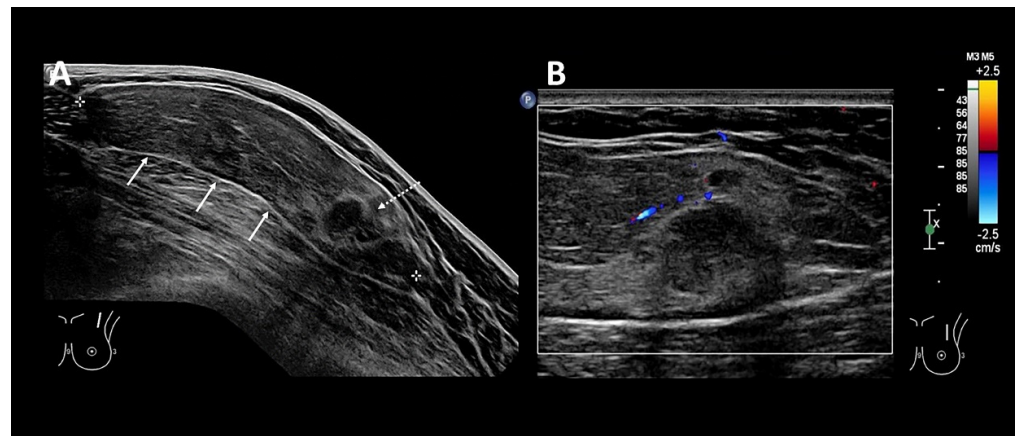


Figure 1. A 50-year-old woman with no past medical history presented with a left anterior chest wall mass. Clinically, the mass was soft, mobile, and non-tender. (A): US image of the left anterior chest wall mass shows a wider than tall mass with well-circumscribed margins (bold arrows). It contains internal fat echogenicity and is in keeping with a fat-containing lesion (i.e., lipoma). Within the inferior portions (dotted arrow), there are focal “mass-like” hypoechoic nodules seen, which are surrounded by a hyperechoic capsule. (B): Doppler US of the focal “mass-like” nodules performed, demonstrated mild increased peripheral vascularity around the hyperechoic capsule but no increased vascularity within the hypoechoic “mass-like” nodules. Findings were indeterminate for malignant change of a lipomatous lesion.

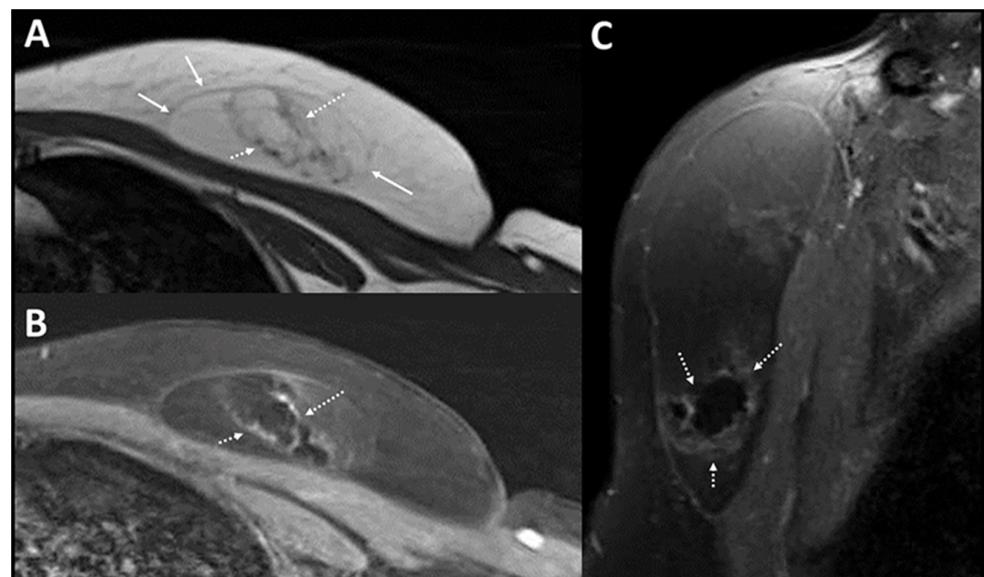


Figure 2. MRI of left anterior chest wall. MRI was performed for the patient in view of possible malignant change (A): Axial T1w image of the left anterior chest wall mass shows a fat-containing lesion in the left anterior chest wall (bold arrows) in keeping with a lipoma. Within the inferior portion, there are fat-containing areas on MRI, which are surrounded by T1w hypointense irregular bands (dotted arrows). (B): These irregular T1w hypointense bands show enhancement on the post contrast enhanced image. (C): Sagittal post contrast enhanced image shows similar findings of irregular rim enhancement around a focal fat-containing central component within inferior portions of the lipoma.

Photoacoustic (PA) tomography, a hybrid optical imaging modality, is based on the light-induced ultrasound waves providing the contrast of optical imaging combined with the high spatial resolution of ultrasound [5]. Its ability to provide the distribution of endogenous chromophores, such as blood oxygenation [6], water [7], lipid [7–10] and

recently collagen [11,12], makes it attractive as a potential adjunct tool to various aspects of ultrasound. This is particularly useful in regions abundant with these chromophores, such as superficial soft tissues and the breast, or in fat-containing and fibrotic/necrotic conditions, such as fat necrosis. However, these theoretical advantages and usages of chromophore differentiations have not been demonstrated in daily clinical usage. Herein, we present interesting images that demonstrate for the first time the biochemical signatures of fat necrosis derived by PA and its agreement with histopathology (Figure 3). A detailed description of PA imaging protocol and image reconstruction is included in Appendix A. This work showcases the potential of PA as an adjunct for US to improve the diagnostic confidence for fat necrosis.

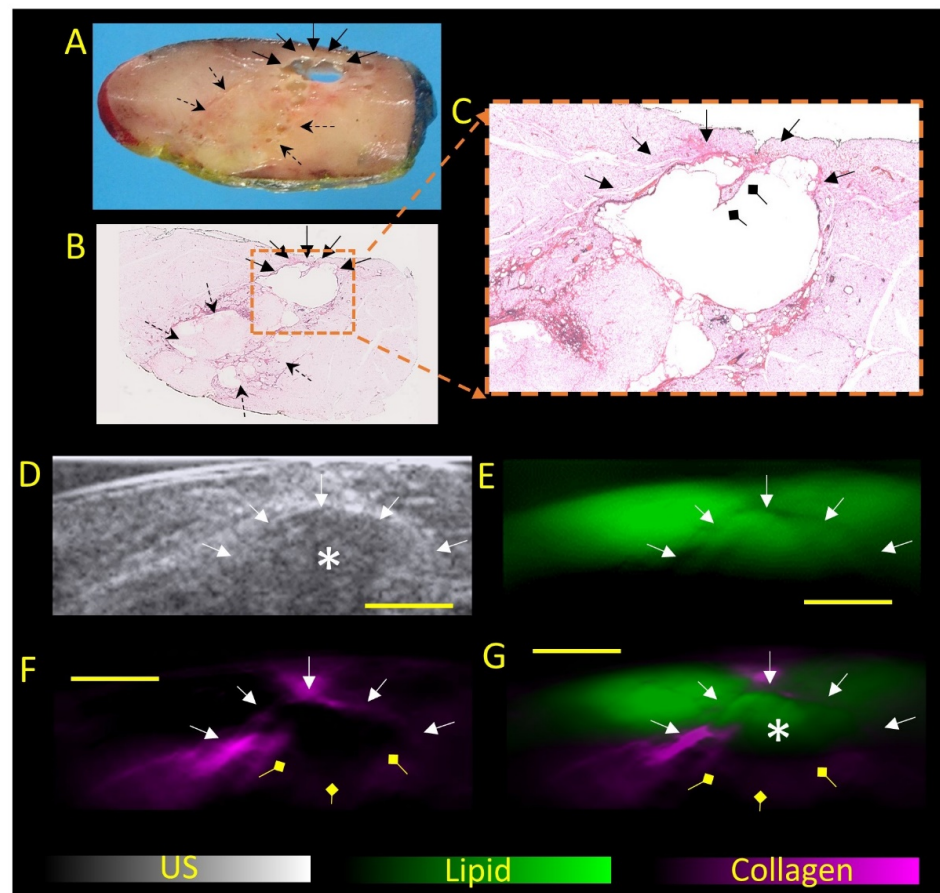


Figure 3. PA imaging of the excised tissue. Patient underwent uneventful excision of the left chest wall mass and was imaged with PA. Methods are as described in Appendix A. (A): Gross pathology of a representative cut section of the lipomatous tumor showing yellowish fatty appearance and foci of necrosis (dotted arrows). Focal cystic change containing oily fluid secondary to fat necrosis was present at where the “mass-like” nodules were seen on US (bold arrows). This area is rimmed by fibrosis. (B): H&E-stained microscopic image of the lipomatous tumor confirms prominent degenerative change, featuring areas of fat necrosis (dotted arrows), cystic change (bold arrows), and fibrosis. (C): shows zoomed in image of the cyst with septation (diamond arrow). This largest area of cystic change (bold arrows) corresponds to the “mass-like” nodule as seen on ultrasound (labelled as *). (D): The “mass-like” nodule near the posterior margin (*), surrounded by a hyperechoic rim (bold arrow), was targeted for PA imaging. Corresponding PA images showing distribution of lipid (E) and collagen (F), or their overlay (G) demonstrated collagenous signal corresponding to the hyperechoic halo in keeping with fibrosis. Within the “mass-like” region, the imaged portions demonstrated lipid signal, which was similar in intensity to the surrounding lipoma. No suspicious fat or collagenous-replacing masses were identified. No blood signals were obtained from this ex vivo study as there was no active ongoing blood flow after lesion excision. Scale bar 5 mm.

In this case, the authors have successfully demonstrated biochemical features of fat necrosis on PA as a first in-human demonstration with histopathological correlation. PA was able to identify the “mass-like” hypoechoic regions on US as fat-containing, rather than fat-replacing. On pathology, the lipid signals on PA correspond to liquefied necrotic fat from cystic degeneration, while the collagen signals on PA correspond to the fibrosis around the cavity. Hence, the biochemical capability of fat and collagen characterization could help to resolve ambiguous findings on US and improve diagnostic confidence for fat necrosis.

As it is crucial to obtain pathological correlation with US-PA images, excised tissues with no active blood signals had to be obtained. The authors believe the incorporation of blood signals in in vivo imaging would further intensify our understanding of the pathophysiology and respective imaging correlations for fat necrosis. Although the results from a single case may seem promising, more work must be done to validate these findings. In particular, more work must be done to validate findings of benign lipomas, fat necrosis, and malignant lipomatous tumors to investigate their biochemical differences. With more data, PA could potentially translate downstream into clinical imaging workflows for better characterization of superficial/breast lumps where fat-containing lesions are common. However, for widespread clinical adoption, there needs to be vast improvements in both hardware and software for PA imaging to improve its imaging depth (to at least 3–4 cm), its field of view, as well as spectral coloring.

Author Contributions: Conceptualization, Y.G.; methodology, Y.G., G.B., H.M.T., C.W.Q.N., E.F., R.B., M.H., S.W.T., C.W.C., M.H., T.C.P., S.A.B. and Y.T.L.; software, Y.G., G.B. and H.M.T.; writing—original draft preparation, Y.G.; writing—review and editing, Y.G., G.B. and H.M.T.; supervision, M.O. and S.T.Q. All authors have read and agreed to the published version of the manuscript.

Funding: This research was funded by (1) Agency of Science, Technology and Research (A*STAR), under its BMRC Central Research Fund (UIBR) 2021 and (2) NMRC clinician-scientist individual research grant new investigator grant (CS-IRG NIG).

Institutional Review Board Statement: The study was conducted in accordance with the Declaration of Helsinki and approved by the Institutional Review Board (or Ethics Committee) of NATIONAL UNIVERSITY HOSPITAL, SINGAPORE (2017/00805, date of approval: 12 October 2017) for studies involving humans.

Informed Consent Statement: Informed consent was obtained from all subjects involved in the study.

Conflicts of Interest: The authors declare no conflict of interest. The funders had no role in the design of the study; in the collection, analyses, or interpretation of data; in the writing of the manuscript, or in the decision to publish the results.

Appendix A

Appendix A.1. Materials and Methods

The excised lipoma was collected fresh from the operating theatre and subjected to US-PA imaging using the commercially available MSOT inVision 512-echo system (iThera Medical GmbH, Munich, Germany), fitted to a customized 2D handheld probe (specifications: 2D array of 256 detector elements (arranged along a 125° arc on a spherical surface: radius 40 mm and 5 MHz centre frequency)). The detector was placed on the inferior portions of the lipoma to image the “mass-like” nodules.

PA images were acquired at near infrared wavelengths—700, 730, 760, 800, 850, 920, 930, 970, 1000, 1050, 1064, and 1100 nm—to allow for deep-tissue imaging. Big differences in absorption of light at these wavelengths by chromophores in breast tissue, such as blood, lipid, and collagen, have aided the unmixing of these chromophores. Data were processed using ViewMSOT 3.8 software (Release 3.8, Munich, Germany) and reconstructed using the backprojection algorithm, after applying a bandpass filter with cut-off frequencies of

50 kHz and 6.5 MHz. The distribution of collagen and lipid were visualized through spectral unmixing of the reconstructed data.

References

1. Genova, R.; Garza, R.F. *Breast Fat Necrosis*; StatPearls Publishing: Treasure Island, FL, USA, 2022.
2. Chan, L.P.; Gee, R.; Keogh, C.; Munk, P.L. Imaging features of fat necrosis. *AJR Am. J. Roentgenol.* **2003**, *181*, 955–959. [[CrossRef](#)] [[PubMed](#)]
3. Taboada, J.L.; Stephens, T.W.; Krishnamurthy, S.; Brandt, K.R.; Whitman, G.J. The many faces of fat necrosis in the breast. *AJR Am. J. Roentgenol.* **2009**, *192*, 815–825. [[CrossRef](#)] [[PubMed](#)]
4. Fernando, R.A.; Somers, S.; Edmonson, R.D.; Sidhu, P.S. Subcutaneous fat necrosis: Hypoechoic appearance on sonography. *J. Ultrasound Med.* **2003**, *22*, 1387–1390. [[CrossRef](#)] [[PubMed](#)]
5. Beard, P. Biomedical photoacoustic imaging. *Interface Focus* **2011**, *1*, 602–631. [[CrossRef](#)] [[PubMed](#)]
6. Li, M.; Tang, Y.; Yao, J. Photoacoustic tomography of blood oxygenation: A mini review. *Photoacoustics* **2018**, *10*, 65–73. [[CrossRef](#)] [[PubMed](#)]
7. Diot, G.; Metz, S.; Noske, A.; Liapis, E.; Schroeder, B.; Ovsepian, S.V.; Meier, R.; Rummeny, E.; Ntziachristos, V. Multispectral Optoacoustic Tomography (MSOT) of Human Breast Cancer. *Clin. Cancer Res.* **2017**, *23*, 6912–6922. [[CrossRef](#)] [[PubMed](#)]
8. Balasundaram, G.; Goh, Y.; Moothanchery, M.; Attia, A.; Lim, H.Q.; Burton, N.C.; Qiu, Y.; Putti, T.C.; Chan, C.W.; Hartmann, M.; et al. Optoacoustic characterization of breast conserving surgery specimens—A pilot study. *Photoacoustics* **2020**, *19*, 100164. [[CrossRef](#)]
9. Lei, P.; Hao, J.; Wang, L.; Wen, X.; Xiong, K.; Zhang, P.; Zhang, L.; Yang, S. Reliability assessment on intravascular photoacoustic imaging of lipid: Ex vivo animal and human sample validation. *J. Biophotonics* **2020**, *13*, e202000162. [[CrossRef](#)] [[PubMed](#)]
10. Zhang, J.; Yang, S.; Ji, X.; Zhou, Q.; Xing, D. Characterization of lipid-rich aortic plaques by intravascular photoacoustic tomography: Ex vivo and in vivo validation in a rabbit atherosclerosis model with histologic correlation. *J. Am. Coll. Cardiol.* **2014**, *64*, 385–390. [[CrossRef](#)] [[PubMed](#)]
11. Goh, Y.; Balasundaram, G.; Tan, H.M.; Putti, T.C.; Tang, S.W.; Ng, C.W.Q.; Buhari, S.A.; Fang, E.; Moothanchery, M.; Bi, R.; et al. Biochemical “decoding” of breast ultrasound images with optoacoustic tomography fusion: First-in-human display of lipid and collagen signals on breast ultrasound. *Photoacoustics* **2022**, *27*, 100377. [[CrossRef](#)]
12. Regensburger, A.P.; Fonteyne, L.M.; Jüngert, J.; Wagner, A.L.; Gerhalter, T.; Nagel, A.M.; Heiss, R.; Flenkenthaler, F.; Qurashi, M.; Neurath, M.F.; et al. Detection of collagens by multispectral optoacoustic tomography as an imaging biomarker for Duchenne muscular dystrophy. *Nat. Med.* **2019**, *25*, 1905–1915. [[CrossRef](#)] [[PubMed](#)]